PCIM Europe 2022; International Exhibition and Conference for Power Electronics, Intelligent Motion, Renewable Energy and Energy Management; Proceedings of

Inductive Power Transfer System for Auxiliary Power Supply in Medium Voltage Converters

X. Du, C. Li, and D. Dujic

POWER ELECTRONICS LABORATORY
ÉCOLE POLYTECHNIQUE FÉDÉRALE DE LAUSANNE

PCIM Europe 2022, 10 – 12 May 2022, Nuremberg DOI:10.30420/565822105

Inductive Power Transfer System for Auxiliary Power Supply in Medium Voltage Converters

Xiaotong Du, Chengmin Li, Drazen Dujic

École Polytechnique Fédérale de Lausanne (EPFL), Power Electronics Laboratory, Switzerland

Corresponding author: Xiaotong Du, xiaotong.du@epfl.ch

Abstract

Inductive power transfer technology is an attractive solution for medium voltage applications by eliminating the need for high voltage cables or wired connections in general. This paper introduces an inductive power transfer system which has multiple independent coil-rectifier outputs, multiple series connected transmitter coils and are supplied from a single transmitter-side converter. Due to the high insulation capability between transmitter and receiver coils, presented system is conceived to be used as auxiliary power supply for power electronics building blocks in medium voltage converters. The coil geometry, compensation network and power electronic converters are designed to achieve high power density and efficiency, despite the large distance between coils that must be overcome. Experimental test setup with five coil pairs is used to demonstrate performances of the system.

1 Introduction

Power electronics building block (PEBB) as a fundamental block in modular converters is an established approach, as way to serve various applications by integrating power devices, gate drivers, sensors and other components together into fundamental building block with well defined interfaces. All these functional components need to be energized, therefore auxiliary power supply (APS) which provides energy to those units is indispensable in a PEBB structure.

For multilevel converters, APS itself could be powered from the inside of the submodule (internal APS) [1] or from an external low voltage supply on ground potential (external APS) [2]. Both of these solutions are widely deployed in commercial medium voltage products, each offering their pros and cons.

The input of internal APS is directly connected to the DC-link capacitor inside the submodule. Typically a Flyback designed to operate with large input voltage range and with multiple outputs is used [1], but other converter topologies are possible as well. On contrary, external APS realizes the independent operations since it is fed from an independent external grid power source [3]. In the start-up and fault-diagnosing period, the external APS system operates normally to assure that the gate driving, communication, sensing and fault detection circuits are always enabled.

One of the biggest problem the external APS faces, in medium voltage applications, is the high insulation requirement between its input and output [4] (1-36 kVac for medium voltage converters), since its input is connected to external grid power source on approximately ground potential and its output is floating and could reach the working voltage of the entire converter. Even though realizing high insulation with traditional transformers is simple and possible, with requirement of small power transmission, the conventional transformers become rather bulky and costly. Therefore it is beneficial to look for alternative solutions. The wireless inductive power supply without physical contact between the primary and receiver sides is suitable for this application. An inductive power transfer (IPT) system consists of the transmitter coils and the receiver coils, which can be interconnected in different ways.

There exist several solutions supplying PEBBs with galvanically isolated outputs based on IPT. The transmitter side can have a single converter and a common current wire loop through receiver coils or

ISBN 978-3-8007-5822-7

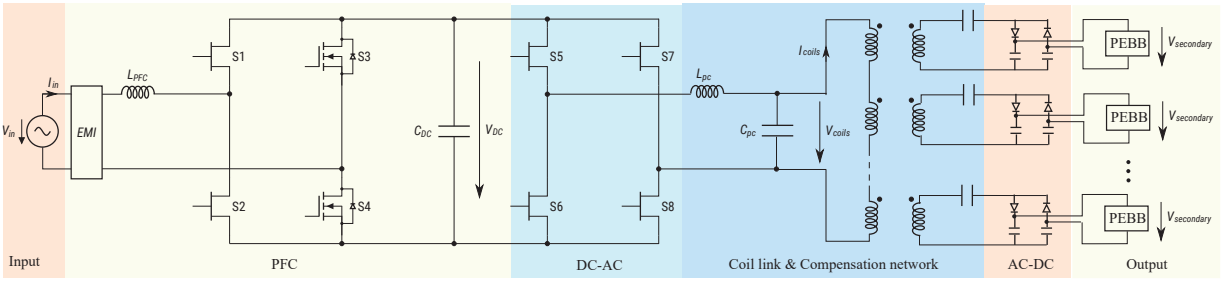

Fig. 1: The auxiliary power supply for PEBBs using IPT technology. Transmitter coils are connected in series and receiver coils are supplying modular PEBBs with independent outputs.

separate converters with separate transmitter coils [5] supplying different receiver coils. The transmitter and receiver coil can also be integrated on a single PCB [6]. However, in all of these solutions, the receiver cannot be completely physically separated from the transmitter, nor can coil pairs work independently without affecting the normal operation of other coils.

In this paper, an IPT system based on planar PCB coils is designed as a solution of APS for PEBBs. The entire IPT system is shown in Fig. 1, where multiple transmitter coils are connected in series with single phase supply through a power factor correction (PFC) and an inverter stage. Receiver coils are independent and each coil is supplying one PEBB through a passive rectifier. Transmitters and receivers are insulated only by air or other insulating material applied directly to coils. The LCL-S compensation network is selected to achieve independent outputs among receiver coils, ensuring that the output voltage on each load is not affected by the condition of other loads [7].

The prototype system in this paper has specifications as listed in Tab. 1. The PFC specifications are selected to comply with the commercially adopted PFC converters and switching frequency is selected as 65 kHz. The rated output voltage of the secondary side is selected as 36 V DC. In reality, owing to the non-ideal factors of the parameters of the components, it is considered that additional non-isolated DC-DC converter is present in the PEBB for tight voltage regulation, thus removing the need from the IPT system to provide fine regulated output voltage to simplify the inverter stage structure. The output power of each stage is selected as 150W, considering the auxiliary power need for the cooling and other components in each PEBB. It should be pointed out that the above mentioned parameters are taken as a typical application scenario for conducting the optimization in the following sections.

Tab. 1: Design specifications for IPT system

Input voltage	90-265 V_{AC}
PFC switching frequency	65 kHz
Coil pairs in series	5
Coil type	Planar PCB
Output voltage of each coil	36 $\pm$ 2 V
Output (peak) power of each coil	150 W
Insulation voltage	6 kV

2 Coil link design

As demonstrated in Fig. 1, coil link is composed of transmitter side compensation network, transmitter coils, receiver coils and receiver side compensation network. Coil link transfers power from primary side to the secondary side efficiently as well as offering required galvanically isolation.

Firsly, LCL-S compensation topology is selected in order to get constant voltage on coil output despite various load conditions [7]. A highly accurate resonant circuit with high power high frequency capability is needed in order to achieve expected performance of LCL-S compensation network. In this paper, when the prototype coils are mounted and fixed to the position, the inductance of series connected transmitter coils is measured and the transmitter side compensation network is adjusted to compensate the total inductance of transmitter side coils.

In the proposed solution, all the transmitter coils are identical and all the receiver coils are the same.

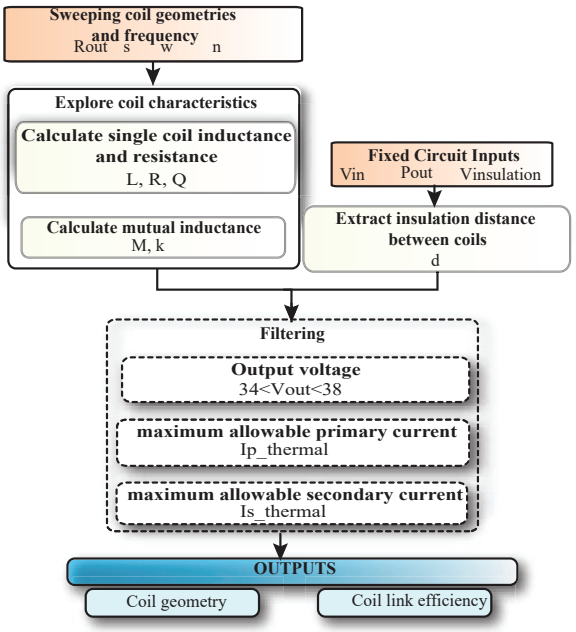

Fig. 2: Approach followed in this paper in order to explore performances of different coil pair geometries.

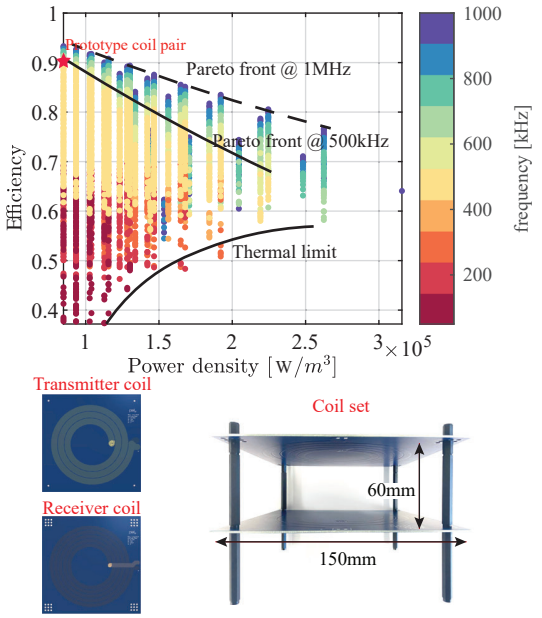

Fig. 3: The figure on top shows Pareto plot of coil link efficiency and power density in the full range of design space. One design at 500kHz operating frequency is selected for prototype and marked as star in the figure. The figure on bottom shows the prototype coils.

However, the transmitter coils are not necessarily identical to receiver coils, offering more degrees of freedom in the design. When it comes to optimize coil pairs, the design approach in Fig. 2 is deployed. Owing to the LCL-S compensation network which maintains a constant current to all the coils, the optimization is done on single coil pair and it leads to optimized 5 coil pairs eventually. The free design parameters are coil geometry parameters and frequency of the excitation. The design space is shown in Tab. 2. The distance between transmitter coil and receiver coil is fixed and defined according to standard IEC 61800-5-1 since transmitter coils and receivers coils are insulated by air only. In the design, 60 mm is taken as insulation distance to fulfill 6 kV system working voltage requirement.

Tab. 2: Design space of PCB coil geometries and operating frequency

Outer radius	10-75 mm
Copper trace width	1-20 mm
Space between turns	1-20 mm
Number of turns	$max = \frac{Rout}{w+s}$
Operating frequency	50-1000 kHz

The coil geometry exploration range is described in Tab. 2. The performance of various coil geometries within the design space are evaluated based on mathematical models presented in details in [8]. Coil geometries are swept to produce a database of coils, which are individually evaluated at first. Then, coils are grouped in pairs and all possible combinations are evaluated considering the key performance indicators, including the coupling factor, self inductance and resistance. Finally, designs are filtered by their output power and voltage requirements.

The trade-off between coil link efficiency and power density is shown in Fig. 3. The coil link efficiency refers to the efficiency from the transmitter coil to the receiver coil excluding losses on the compensation network and power electronics converters. The power density is defined as $\frac{2P_{out}}{(S_p+S_s)d}$, where P_{out} is the output power, S_p and S_s are the surface area of transmitter and receiver coils and d is the distance between two coils. With the Pareto plot, users can choose their final design on the Pareto fronts according to their requirements of efficiency and power density. In this paper, the design with the highest efficiency on the Pareto front of 500kHz

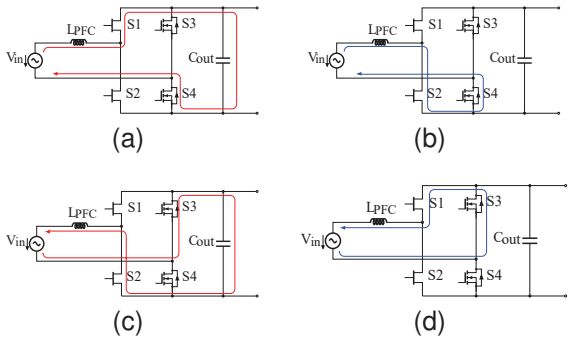

Fig. 4: Conduction paths for the totem-pole PFC. S1 and S2 switch at 65 kHz, S3 and S4 switch at grid frequency. (a) In the positive grid half cycle, S1 operates as boost switch (b) In the positive grid half cycle, S2 acts as synchronous rectifier (c) In the negative grid half cycle, S2 operates as boost switch (d) In the negative grid half cycle, S1 acts as synchronous rectifier.

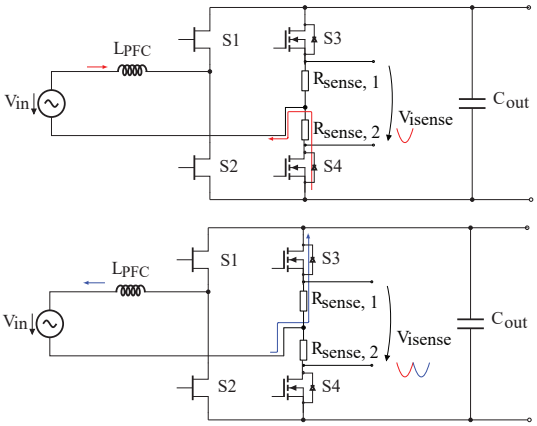

Fig. 5: Inductor current sensing method during the positive and negative half-cycles. Due to this approach, the control circuits for the input stage are referenced to the switching node of the line frequency leg.

is selected and prototyped. The resulting coil PCBs are shown in Fig. 3. The transmitter and receiver planar coils are geometrically different (number of turns, trace width, gap between turns), however both PCBs are designed to square shape of size 150 mm $\times$ 150 mm in order to facilitate mechanical mounting.

3 Transmitter side converter

As demonstrated in Fig. 1, the transmitter side converter is supplied from the standard low voltage distribution network and outputs as a constant voltage source generating $\pm$400 V square wave voltage with 50% duty cycle and 500 kHz frequency. The AC-AC converter has two stages including the PFC stage regulating input to 400V DC and open-loop full bridge inverter stage supplying primary coils. GaN devices are applied for both Totem-pole PFC and inverter in favor of low loss and compact design.

3.1 Totem-pole PFC

Comparing to conventional Boost PFC, totem-pole PFC reduces the conduction losses by having only two devices conducting at any time. Gallium Nitride (GaN) normally off High Electron Mobility Transistor (HEMT) devices don't have reverse recovery losses which make them suitable for use as Boost switches.

The working logic of totem-PFC is shown in Fig. 4. Similar to the boost converter, the main inductor L_{PFC} is either releasing energy to the load (red paths) or storing energy from the source (blue paths). S1 and S2 are commutating at high switching frequency, while S3 and S4 switch at line frequency. In this work, two enhancement mode GaN HEMTs IGO60R070D1 from Infineon (S1 and S2 in Fig. 4) and two silicon switches IPT65R033G7 MOSFET from Infineon (S3 and S4 in Fig. 4) are used as low switching frequency devices. Design from Infineon [9] is used as reference and component dimensioning are done to meet requirement of IPT system.

There are no commercial specific controller for totem-pole PFC, the controller ICE3PCS01G designed for Boost PFC is used in the design. There are two main considerations to adapt this controller in totem-pole PFC: sampling of AC current and four signal generation from a single PWM ouput. Firstly, the totem-pole PFC has the inductor on the AC side. In order to measure the inductor current regardless of the grid voltage polarity, two current sensing resistors are placed on the MOSFET leg of the converter to reconstruct the AC current, with the control ground referenced to the switching node [9], as demonstrated in Fig. 5.

The second adaptation is creating the four gate signals for the totem-pole PFC from a single PWM signal. Additional logic is required to generate PWMs for the four switches. Firstly, the grid voltage po-

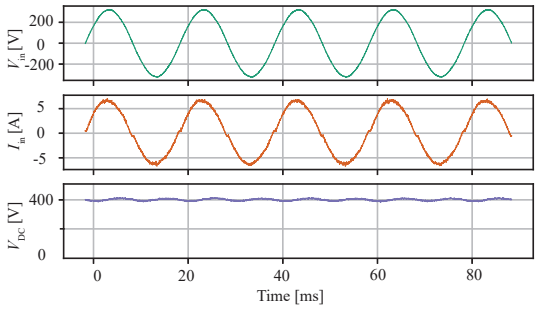

Fig. 6: Operation of PFC at nominal input voltage and 600 W load. From top to bottom: input single phase voltage; input current; DC bus voltage.

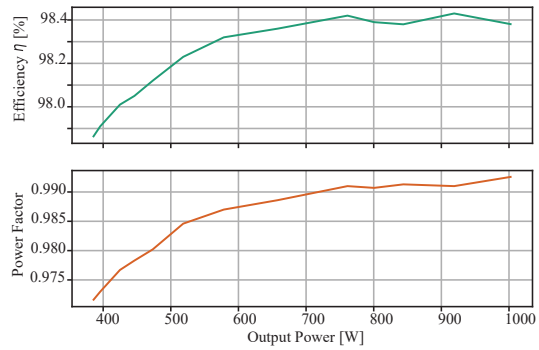

Fig. 7: PFC stage efficiency and power factor under different loads.

larity is detected with zero-crossing detection. The line-frequency MOSFETs (S3, S4) will simply commutate based on the polarity of the voltage and GaN devices will operate as boost switch or synchronous rectifier depending on the polarity of grid voltage. Secondly, the PWM signals of GaNs (S1, S2) are generated by PWM signal of the chip, with deadtime inserted.

In order to verify the unity power factor, input current THD and constant DC link voltage, Fig. 6 shows the waveforms at nominal input voltage and 600 W load. The input current THD was computed offline to be 3.51%. Both the efficiency and the power factor of the PFC stage were measured and recorded for different output power, and the results are shown in Fig. 7. The unity power factor is guaranteed and is better for higher power. The power factor at 600 W is computed to be 0.987. The efficiency measurements show the advantage of using the GaN based totem-pole topology, with a measured peak efficiency of above 98.4%.

3.2 Inverter stage

For an available DC voltage of 400 V, full bridge (FB) topology is expected to improve the efficiency of the system [7]. With the adoption of LCL-S network, the control of the inverter can be greatly simplified. The output of the inverter stage is a 50% duty cycle square wave at 500 kHz.

The thermal design of GaN devices is important under 500 kHz switching frequency. In this paper, two measures are deployed to avoid overheating of GaN devices. Firstly, the devices are switched at zero voltage. This is realized by bringing the compensation inductance slightly higher than the transmitter coil inductance which will together appear as an inductive load to the converter. Secondly, a heatsink with an integrated 5 V fan that ensures a thermal resistance of 1.95°C/W is mounted on the bottom side of GaN devices, which would keep the worst-case junction temperature at 76.7°C when soft switching is guaranteed.

Even the inverter operates at open loop, the over current protection and soft start is still required to avoid the excessive stress of the GaN devices. In this work, LTC1922-1 from Analog Devices is used as PWM controller which integrates the soft-start and load over-current protection functions.The soft start is realized by gradually increasing the phase shift angle among the two phase legs. The current protection is realized by monitoring a voltage from the current measurement on the CS pin. A 1:100 turns ratio current sense transformer is used with its primary side measuring the current through the transmitter compensation inductor, and its secondary side connecting to a rectifier and a sensing resistor of 2.7 Ω in order to set peak current limit to 15 A.

When the DC link capacitor is sufficiently charged, the PFC controller will regulate DC link voltage to the nominal value 400 V and only after this the inverter stage starts modulating. To enable this, auxiliary supply for the inverter stage will be only activated when the DC link voltage reaches nominal value. The final design of primary side converter is shown in Fig. 8. In the proposed design, the PFC controller and auxiliary power supply is placed on a separate boards to reduce the surface of the converter. The PFC and inverter are placed together on a power board. To realize the flexible adjustment of the compensation network, another board for the

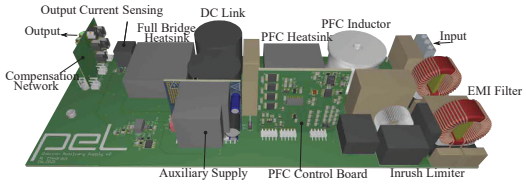

(a)

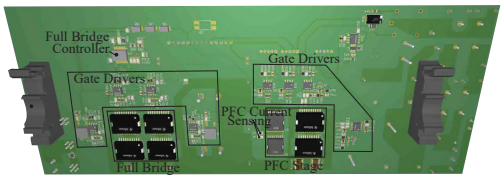

(b)

Fig. 8: (a) Top and (b) bottom views of the transmitter side converter.

Tab. 3: Self and mutual inductance under 60 mm air gap between transmitter and receiver coils

	Without ferrite	With ferrite
L_t	1.12 µH	1.9 µH
L_r	3.02 µH	4.9 µH
M	0.274 µH	0.557 µH
$k = \frac{M}{\sqrt{L_t L_r}}$	0.15	0.18

compensation network is plugged on the output of the inverter.

4 Receiver side rectifier

For the IPT system, the output DC voltage depends on having a full bridge or half bridge topology. The passive half bridge is used on receiver output stage [7]. The schottky diodes STPS30M100DJF-TR with rating 100V 30A are used to achieve low losses. The capacitor is sized to limit the voltage ripples on output voltage. With nominal output ratings, 15 µF MLCC capacitors with voltage rating of 600 V are used to limit voltage ripple within 5%.

5 Experimental test

The coils are firstly characterized with BK895 LCR meter with and without ferrite (3F36) on the back-side of coils. The inductance as well as coupling factor are shown in Tab. 3. With different distance between transmitter and receiver coil, the coupling

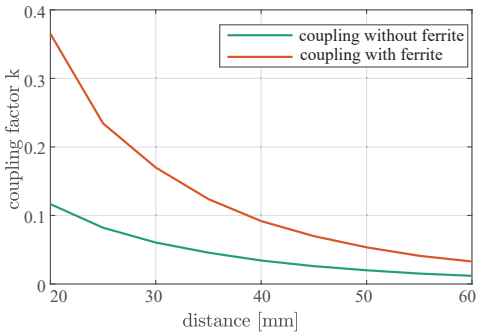

Fig. 9: Coupling factor between transmitter and receiver coils as distance changes.

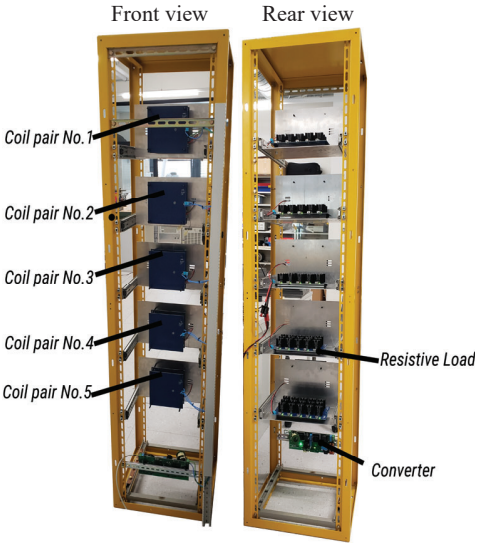

Fig. 10: IPT system test set up including PFC, DC-AC inverters, compensation networks, coil links, rectifiers and resistive loads. Five IPT coils pairs have their transmitter coils connected in series and receiver coils connected to independent loads.

factor is changing as shown in Fig. 9. It can be seen that decreasing distance and adding ferrite can increase coupling factor of coils.

The power tests are done with test set up in Fig. 10 for both conditions: without ferrite and with ferrite, respectively. Five pairs of coil are installed on five stacked drawers and the distance between transmitter and receiver coils are controlled by the drawer which allows distance range from 0 mm to over 300 mm. Such configuration is similar to the application scenario where PEBBs are installed and externally supplied. The five transmitter coils get power from a single transmitter side converter. During the test, the distance between transmitter coil and receiver

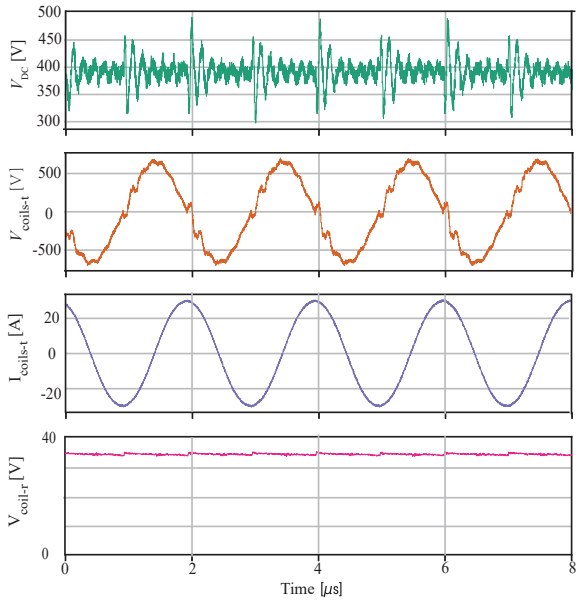

Fig. 11: Test results without ferrite. From top to bottom: input DC voltage before the inverter; voltage across the five series connected transmitter coils; current through transmitter coils; output DC voltage at the load side of coil pair No.3.

coil is fixed to 60 mm. The resistive load on each receiver side is 10 Ω realized as resistive switchable load bank. At the end of this section, with the switchable load bank, the test with load change on one coil pair is done to verify the independent outputs of proposed IPT system.

5.1 Test without ferrite

The coil geometry was optimized for the coils without ferrite condition following the design procedure in Section 2. In order to verify that coils without ferrite on their backside is able to transfer 100 W overcoming 60 mm distance, the power test has been done and the test results are shown in Fig. 11. The output voltage is around 33 V and 108 W is transferred to each load. The voltage ripple is less than 5% of nominal value. The disturbance observed on the voltage across transmitter coils are due to the measurement noises since the current through transmitter coils is rather clean. Comparing to DC link voltage of PFC in no load condition in Fig. 6, a larger disturbance on the DC link voltage is observed here, which is possibly caused by coupling of measurement noise.

Fig. 12: A PCB coil in customized box with ferrite plate on its backside.

5.2 Tests with ferrite

In practice, ferrite is widely adopted in IPT system in order to increase the coupling by reducing leakage magnetic flux and reduce the transmitter side current at the same output power condition. However, when a large air gap is presented for small coil surface areas, the potential gaining benefit is not clear yet. It is worth the effort to investigate the influence of adding ferrite on the back side of the coils.

With the same insulation distance of 60 mm, the coils are tested with ferrites on the backside of both transmitter and receiver coils. As shown in Fig. 12, 2×3 ferrite blocks PLT64-50-5 of material 3F36 from Ferroxcube forms a rectangular plate of $128mm \times 150mm \times 5mm$. The air gap between ferrite blocks and the gap between coil and ferrite are as small as to be negligible. The inductance and coupling factor of coils with ferrite are shown in Tab. 3.

The power test is done with ferrite within the same test setup in Fig. 10. The test result is shown in Fig. 13. It can be seen that the current through transmitter coils is lowered by 30%. This is because with LCL-S compensation network, the current through transmitter coils is $I_t = \frac{U_{in}}{j\omega L_{tot}}$. Since the total inductance of transmitter coils is increased by adding ferrite, under the same input voltage, the current through transmitter coils is decreased. But at the same time, adding ferrite increases the coupling between transmitter and receiver coils and as the result, the output voltage would increase. However, the test only get a slight increase on output voltage on the same coil pair. The increase of output voltage is not as significant as the increase in coupling factor due to two reasons. Firstly, the ferrite on the back side of coils influence the magnetic field inside coil turns and thus increases the coil resistance. Secondly, the components of compensation network is not optimized in this paper, which

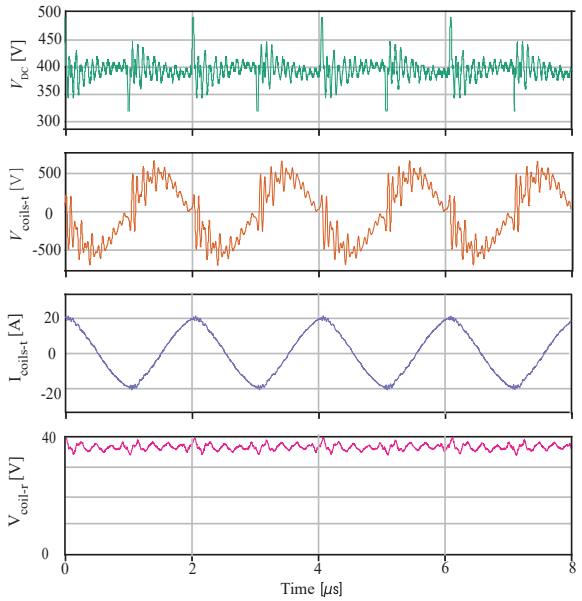

Fig. 13: Test results with ferrite on the backside of both transmitter and receiver coil. From top to bottom: input DC voltage before the inverter; voltage across the five series connected transmitter coils; current through transmitter coils; output DC voltage at the load side of coil pair No.3.

could cause extra loss.

In general, although the coupling factor is slightly increased, adding ferrite on the back side is still beneficial for reducing the power loss and increase the voltage. Or put it in another way, higher power density can be achieved at the same output power condition. However, more work should be conducted to comprehensively taken the influence of ferrite into consideration. In the following experiments, only results with ferrite are demonstrated.

5.3 Test under load change condition

One of the critical design consideration of the auxiliary power system is the ability to generate load independent output voltages. The application of LCL-S compensation network ensures independent operation of each coil pair and realizes stable output voltage on each load despite of load change on other receiver coils. This is verified by a test with load change on one receiver coil in Fig. 10.

During the test, at time t0, the test set up is powered on with full load at each receiver coil. At time t1, the resistive load of coil pair No.3 is fully removed. At no load condition, the voltage of coil No.3 jumps to 60 V, which is nearly $\sqrt{2}$ of the nominal value. In

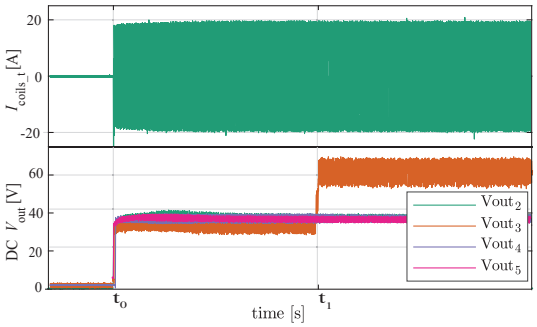

Fig. 14: From top to bottom: current through transmitter coils; output DC voltages from the second coil to the fifth coil.

practice, in order to avoid the high output voltage at no load condition, a large resistance is typically added to pull down the output voltage.

The output voltage from four coil pairs (No.2 to No.5) are shown in Fig. 14. As can be seen, the current through transmitter coils and output voltage on other loads (2nd, 4th, 5th outputs) are constant while the 3rd load is removed, which verifies coil pairs have independent outputs.

It can be also seen that another DC/DC stage is required to get a constant DC voltage for the PEBB. Fortunately, there is a wide range of choices of converters/chips in the market to realize such requirement.

6 Conclusion

The IPT system represents an interesting alternative to state-of-the-art power supply solution with high insulation voltage capability. This work presents the design of an entire IPT system including coil link design, GaN-based transmitter side converter, receiver side passive converter. The performances of the IPT system with five coil pairs connected in series on ther primary side are tested in a laboratory test setup, emulating expected conditions inside the medium voltage converter. The influence and preliminary comparison of operation with or without ferrite on the coil backside has been performed. The proposed solution is verified by experiments and will be further reoptimized for integration into the medium voltage converter, providing auxiliary power for PEBBs.

Acknowledgments

The Authors would like to thank Mr. Roberto Chedraui Abud for his work on realization of transmitter side converter.

References

[1] A. Christe, M. Petkovic, I. Polanco, M. Utvic, and D. Dujic, "Auxiliary submodule power supply for a medium voltage modular multilevel converter," *CPSS Transactions on Power Electronics and Applications*, vol. 4, no. 3, pp. 204–218, 2019. DOI: 10.24295/CPSSTPEA.2019.00020.

[2] D. Peftitsis, M. Antivachis, and J. Biela, "Auxiliary power supply for medium-voltage modular multilevel converters," in *2015 17th European Conference on Power Electronics and Applications (EPE'15 ECCE-Europe)*, 2015, pp. 1–11. DOI: 10.1109/EPE.2015.7309388.

[3] B. Wunsch, D. Zhelev, and B. Oedegard, "Externally-fed auxiliary power supply of mmc converter cells," in *2016 18th European Conference on Power Electronics and Applications (EPE'16 ECCE Europe)*, 2016, pp. 1–10. DOI: 10.1109/EPE.2016.7695304.

[4] K. Kusaka, M. Kato, K. Orikawa, J.-i. Itoh, I. Hasegawa, *et al.*, "Galvanic isolation system for multiple gate drivers with inductive power transfer — drive of three-phase inverter," in *2015 IEEE Energy Conversion Congress and Exposition (ECCE)*, 2015, pp. 4525–4532. DOI: 10.1109/ECCE.2015.7310299.

[5] B. Wunsch, J. Bradshaw, I. Stevanović, F. Canales, W. Van-der-Merwe, and D. Cottet, "Inductive power transfer for auxiliary power of medium voltage converters," in *2015 IEEE Applied Power Electronics Conference and Exposition (APEC)*, 2015, pp. 2551–2556. DOI: 10.1109/APEC.2015.7104710.

[6] V. T. Nguyen, G. Veera Bharath, and G. Gohil, "Design of isolated gate driver power supply in medium voltage converters using high frequency and compact wireless power transfer," in *2019 IEEE Energy Conversion Congress and Exposition (ECCE)*, 2019, pp. 135–142. DOI: 10.1109/ECCE.2019.8912184.

[7] X. Du and D. Dujić, "Inductive power transfer system with series connected primary and independent secondary coils," in *IECON 2020 The 46th Annual Conference of the IEEE Industrial Electronics Society*, 2020, pp. 3901–3906. DOI: 10.1109/IECON43393.2020.9254476.

[8] X. Du, C. Li, and D. Dujić, "Design and characterization of pcb spiral coils for inductive power transfer in medium-voltage applications," *IEEE Transactions on Power Electronics*, vol. 37, no. 5, pp. 6168–6180, 2022. DOI: 10.1109/TPEL.2021.3131013.

[9] S. Kampl and R. Garcias, "2500 w full-bridge totem-pole power factor correction using coolgan™," *Reference Design, Infineon*, 2018, Reliability of Electron Devices, Failure Physics and Analysis.